

Advantages of Advanced Slope Stabilization Technology - Tensioned Rock Anchors and Integrated Connection System

^[1]Chen-Ping Tsou*, ^[2]Kun-Ting Chen, ^[3]Wen-Shinn Shyu

^{[1][2][3]}Department of Civil Engineering, National Pingtung University of Science and Technology,

^[1]p11233002@mail.npust.edu.tw, ^[2]kuntingchen@mail.npust.edu.tw, ^[3]wsshuyu@mail.npust.edu.tw

Abstract—Advanced Slope Stabilization Technology, featuring tensioned rock anchors and an integrated connection system, offers a highly effective solution for slope protection and stabilization. This technology employs pre-tensioned rock anchors to apply controlled forces that reinforce slopes, preventing failures caused by soil erosion, seismic activity, or heavy rainfall. The integrated connection system ensures even load distribution, enhancing structural integrity and durability. A key advantage of this system is its adaptability to various geological conditions, making it suitable for diverse environments, from steep mountain slopes to urban infrastructure projects. The pre-tensioning mechanism actively counteracts destabilizing forces, significantly improving slope safety and reducing the risk of landslides. Additionally, the modular design allows for efficient installation and maintenance, lowering both time and costs. The technology's long-term durability minimizes the need for frequent repairs, providing a sustainable and cost-effective solution. Its high load-bearing capacity and resistance to environmental factors ensure reliable performance over time. By enhancing slope stability, this system protects infrastructure, ecosystems, and human lives, making it an ideal choice for modern engineering challenges.

Keywords:Advanced Slope Stabilization, Tensioned Rock Anchors, Integrated Connection System, Slope Protection, Slope Stability, Pre-Tensioned Forces, Load Distribution, Geological Adaptation, Landslide Prevention, Structural Integrity, Cost-Effective Solutions, Long-Term Durability, Environmental Resistance, Engineering Safety.

I. INTRODUCTION

Taiwan is located in the Pacific Rim seismic belt, at the junction of the Eurasian Plate and the Philippine Sea Plate. The continuous orogeny has led to active geological structures, which are prone to various slope disasters such as landslides, landslides, rock debris slides and rockfalls. In addition, Taiwan's terrain is rugged, with mountains accounting for more than three-quarters of the island's area, steep terrain, and young and fragile geological structures, which also increase the potential for disasters. Geographically, Taiwan is located near the Tropic of Cancer and is in the path of typhoons in the northwest Pacific. On average, there are 3 to 4 typhoons each year. Typhoons bring heavy rains, which are not only heavy but also have an astonishing cumulative rainfall [1,2]. They cause slope sliding, landslides, and rockfalls in mountainous areas, and often lead to serious flooding in plain areas. As cities expand and population increases, the available flat land for development and living is limited, and people are gradually moving to hillsides to build their homes, further increasing the risk of disasters. At the same time, to support the development of mountainous areas [3] road transportation facilities are also continuously extended to mountainous areas, making hillside residences and transportation systems more vulnerable to slope disasters and floods during typhoons and heavy rains. Looking back at major natural disasters in Taiwan in recent years [4,5], including Typhoon Herb (1996), the Chi-Chi earthquake (1999), Typhoon Toji (2001), Typhoon Nari (2001), Typhoon Mintoli (2004), Typhoon Sinlakot (2008), Typhoon Morakot (2009), Typhoon Megi (2010) and Typhoon Saula (2012), all of which have had a significant impact on social security and economic development. Climate change exacerbates extreme weather phenomena. In the past decade, the rainfall brought by typhoons invading Taiwan has increased significantly. Especially after the 921 earthquake in 1999, many slope structures in Taiwan were damaged by the earthquake, and the rock mass became looser. Under the influence of extreme rainfall, highway slope disasters

increased significantly. Taking the 2009 Morakot Typhoon as an example, the disaster in southern Taiwan was serious. The accumulated rainfall in the Alishan area of Chiayi on the 5th was nearly 3,000 mm, far exceeding the annual average rainfall in Taiwan (about 2,500 mm). Taiwan's mountainous terrain and frequent seismic activity necessitate robust slope stabilization measures. Traditional methods, reliant on manual monitoring, are labor-intensive and prone to errors. This study introduces an automated system combining pre-tensioned rock anchors with wireless monitoring to enhance slope stability [6,7,8]. The objectives include reducing material usage, shortening construction timelines, and enabling real-time data transmission for proactive hazard management. [9,10]

II. METHODOLOGY

2.1 STUDY AREA

The research was conducted on Hua64 Road in Hualien County (Fig 1), a region prone to landslides and rockfalls due to its geological and climatic conditions. [11]

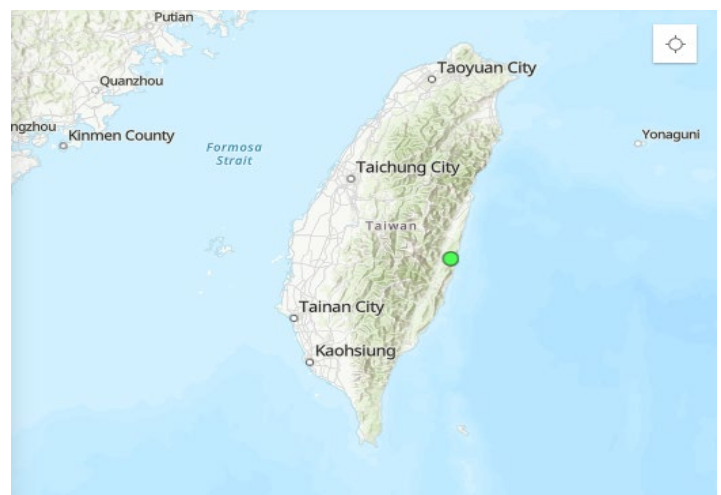


Fig 1 Study Area (TAIWAN)

2.2 Materials and Instrumentation

1. Rock Bolts: Diameter: 25 mm, Cross-sectional area: 506.7 mm², Elastic modulus: 204 kN/mm².(Fig 2)
2. Strain Gauges: Measurement range: ± 3000 kgf/cm², Sensitivity: 0.025% FS.(Fig 3)
3. Calculation of rock bolt pull-out resistance

$$T_u = \pi \cdot D \cdot L \cdot \tau + A \cdot c \dots \dots \dots (1)$$
 T_u : Extreme pull-out resistance (kN)
 D : Bolt drilling diameter (m)
 L : Anchor segment length (m)
 τ : The average bond strength of the rock and soil mass and the grouting body (kPa)
 A : The bearing area at the end of the anchor section (m²)
 c : Compressive strength of rock and soil (kPa)
Refer to : FHWA-IF-99-015 《Ground Anchor Technology》
4. Monitoring System: Automated sensors, solar- powered equipment, and 4G transmission modules for real-time datacollection.(Fig4,5)

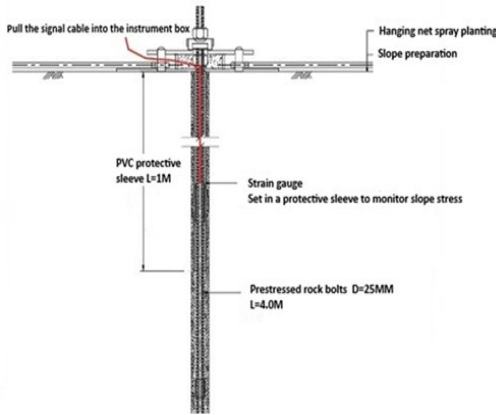


Fig 2 Prestressed rock bolt structure diagram

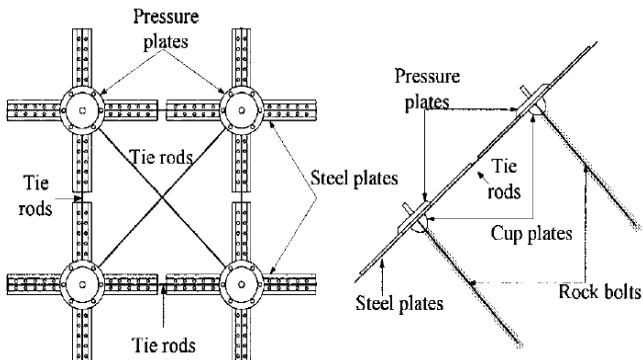


Fig 3 Schematic diagram of the composition of the pre-force rock bolt and the connection system



Fig 4 Solar powered and battery equipment: 1 location

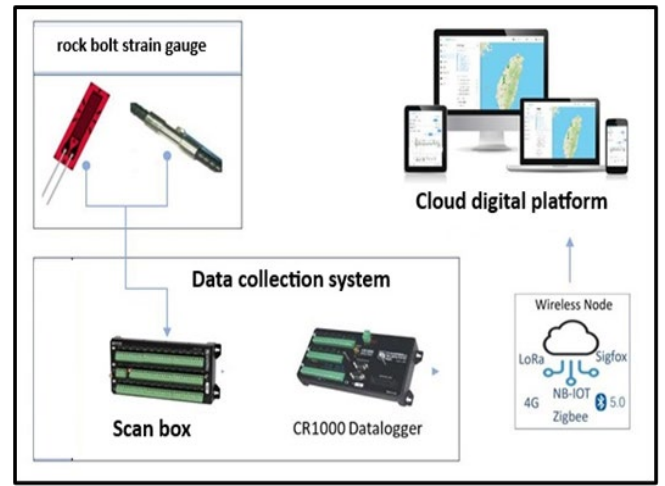


Fig 5 Automated monitoring system architecture diagram

2.3 Monitoring Protocol

Initial Setup: Pre-tension applied: 30 kN.

Time intervals for observations and instrument setting values.

- (1) Installation location of the rock bolt stress sensor (strain gauge): Instruments numbered RS-1 to RS-13, a total of 13 sets. Detailed locations are specified in Fig6 and 7.
- (2) Applied pre-tension value: 30 kN (3T). shown as Table 3
- (3) Measurement instrument used: Automated reading Equipment(Fig 8), see Table 1 for details shown as (Table 1 ,2)
- (4) Initial value establishment date: : October 27, 2022 .



Fig 6 West Side Rock bolt stress sensor (stress gauge): 10 sets

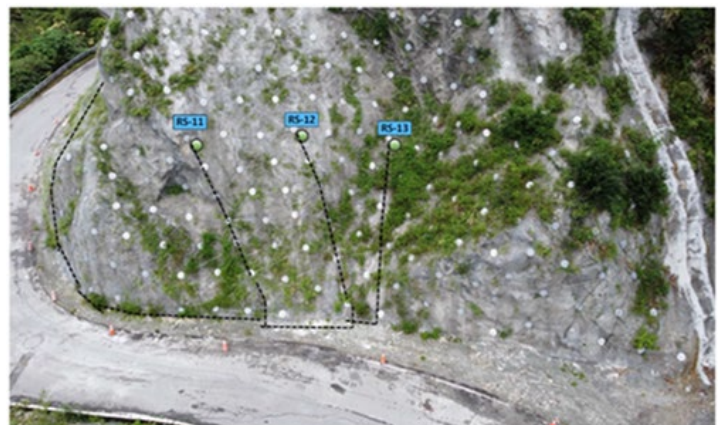


Fig 7 East Side Rock bolt stress sensor (stress gauge): 3 sets

Table 1 List of the number of automated monitoring systems

Instrument name ^⓪	Brand and mode ^⓪	Quantity ^⓪
Rock bolt stress sensor ^⓪ (strain gauge) ^⓪	GeoStar Model 9011 ^⓪	13 Set ^⓪
Data Recorder ^⓪	Campbell Scientific CR300 ^⓪	1 Set ^⓪
Vibrating wire module ^⓪	GeoStar CLK-1 ^⓪	1 Set ^⓪
Multi-function scanner ^⓪	GeoStar M1632 ^⓪	1 Set ^⓪
4G transmission module ^⓪	INM 4G Modem ^⓪	1 Set ^⓪
Solar power supply and battery	GeoSupply P050 Series ^⓪	1 Set ^⓪
Automated database and software ^⓪	GeoSupply Cloud monitoring platform ^⓪	1 type ^⓪

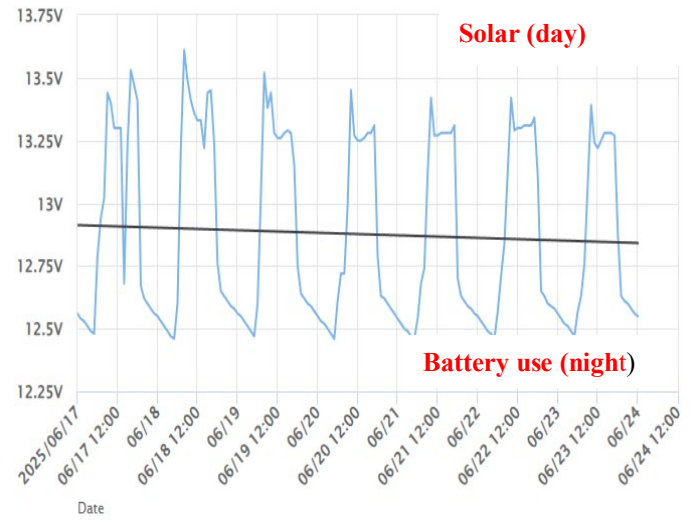


Fig 9 changes in battery Level

Table 2 Overview of Automated Monitoring System Specifications

Instrument name ^⓪	Instruments Specifications ^⓪
Rock bolt stress ^⓪ sensor (strain gauge) ^⓪	(a) Measurement range: $\pm 300\text{kgf/cm}^2$ ^⓪ (b) Sensitivity: $0.025\%\text{FS}$ ^⓪ (c) Non-linearity: $<0.5\%\text{FS Kg/cm}^2$ ^⓪
Data Recorder ^⓪	(a) Number of channels: It has 6 single-point sensor channels or 3 differential sensor channels ^⓪ (b) External channels: can connect to 1 set of 32-channel multi-function scanning box for vibrating wire and temperature measurement or electronic measurement (c) AD resolution: 24bit ^⓪
Vibrating wire module ^⓪	(a) Frequency scanning range: $400 \sim 6000\text{ Hz}$ ^⓪ (b) Accuracy: 0.5 Hz ^⓪ (c) Operating voltage: DC 12V ^⓪ (d) Operating temperature: -
Multi-function scanner ^⓪	(a) Number of connections: 16 single-point sensor channels or 32 differential sensor channels ^⓪ (b) Operating voltage: DC 11V \sim 14V, 0.1A. ^⓪ (c) Operating voltage: DC 11V \sim 14V, 0.1A. ^⓪
4G transmission module ^⓪	(a) Channel: 4G 900/1800/2600 MHz ^⓪ (b) Output: 1 RS232 and 1 RS485. ^⓪ (c) Voltage input: $9 \sim 32\text{ Vdc}$ ^⓪ (d) Operating temperature: -35°C to 75°C ^⓪
Solar power supply ^⓪ and battery equipment ^⓪	Battery: (a) Voltage: 12V (b) Amp hour: 45AH ^⓪ Solar panel: ^⓪ (a) Maximum power: 50W ^⓪ (b) Maximum power voltage: 18V ^⓪ (c) Maximum power current: 2.7A ^⓪ (d) Open circuit voltage: 21.5V ^⓪ (e) Short circuit current: 2.99A ^⓪ (f) Module conversion efficiency: $\pm 3\%$ ^⓪



Fig8 Automatic monitoring system reading record equipment

Table 3: Instrument Initial Values and Coefficients

Instruments number ^⓪	Serial number	Initial pre-tension ^⓪	Initial value ^⓪	Manufacturer's calibration ^⓪ coefficient ^⓪	Management value ^⓪
		Ton ^⓪	digit ^⓪	$\mu\text{E}/\text{digit}$ ^⓪	Ton ^⓪
RS-1 ^⓪	53861 ^⓪	3 ^⓪	6382.703 ^⓪	0.50432 ^⓪	2.1 ^⓪
RS-2 ^⓪	53862 ^⓪	3 ^⓪	6540.632 ^⓪	0.50008 ^⓪	2.1 ^⓪
RS-3 ^⓪	53863 ^⓪	3 ^⓪	6429.819 ^⓪	0.49867 ^⓪	2.1 ^⓪
RS-4 ^⓪	53864 ^⓪	3 ^⓪	6491.384 ^⓪	0.50049 ^⓪	2.1 ^⓪
RS-5 ^⓪	53865 ^⓪	3 ^⓪	6798.764 ^⓪	0.51017 ^⓪	2.1 ^⓪
RS-6 ^⓪	53866 ^⓪	3 ^⓪	6706.982 ^⓪	0.49860 ^⓪	2.1 ^⓪
RS-7 ^⓪	53867 ^⓪	3 ^⓪	6665.611 ^⓪	0.49466 ^⓪	2.1 ^⓪
RS-8 ^⓪	53869 ^⓪	3 ^⓪	6576.533 ^⓪	0.51262 ^⓪	2.1 ^⓪
RS-9 ^⓪	53870 ^⓪	3 ^⓪	6518.305 ^⓪	0.49298 ^⓪	2.1 ^⓪
RS-10 ^⓪	53871 ^⓪	3 ^⓪	6630.923 ^⓪	0.48500 ^⓪	2.1 ^⓪
RS-11 ^⓪	53872 ^⓪	3 ^⓪	6477.916 ^⓪	0.49564 ^⓪	2.1 ^⓪
RS-12 ^⓪	53873 ^⓪	3 ^⓪	6691.731 ^⓪	0.50817 ^⓪	2.1 ^⓪
RS-13 ^⓪	53874 ^⓪	3 ^⓪	6837.152 ^⓪	0.50562 ^⓪	2.1 ^⓪

(5) Data acquisition interval: From November 1, 2022 to October 30, 2024 .

Prestress Calculation: The strain gauge measures the readings: digit digit=(Hz2/1000) ·It is the original unit of the vibrating string instrument, digit Difference ΔR : ΔR (The observed value -Initial value)

$$(b-a)=\Delta R_1、(c-a)=\Delta R_2、(d-a)=\Delta R_3、(e-a)=\Delta R_4\ldots\ldots (2)$$

The pre-force change is calculated as follows:

$$P=\Delta R \cdot A \cdot E \cdot K \ldots\ldots\ldots (3)$$

ΔR : digit Difference A: Rock bolt fault area

E: Elastic coefficient K: gauge factor

P: Preload variation

The initial applied prestress value is 30 kN.

The current prestress value: $P_x=30+P$ (unit kN)..... (4)

Unit conversion: 1T \approx 10kN

III. Results

3.1 RAINFALL AND SEISMIC

Impact Rainfall: 18 days with precipitation exceeding 50 mm shown as (Fig 10、Fig11)

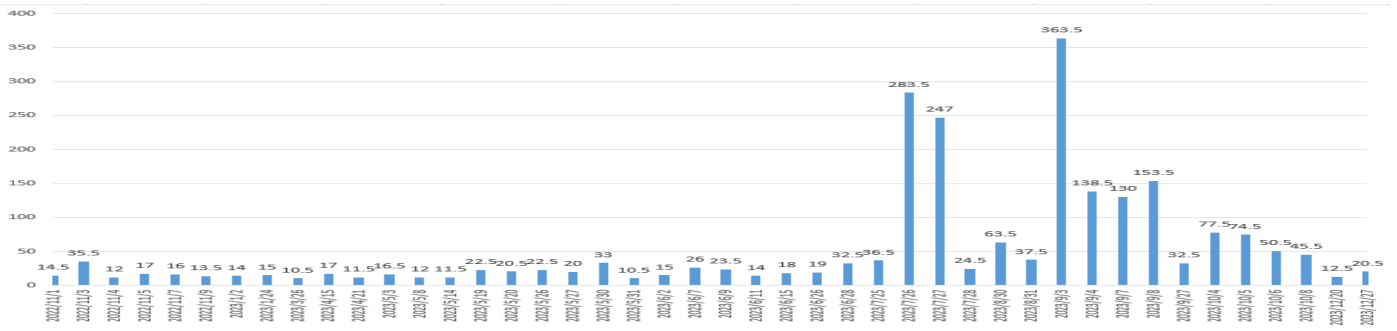


Fig 10: Rainfall Statistics Table from November 2022 to December 2023 Unit: day/mm

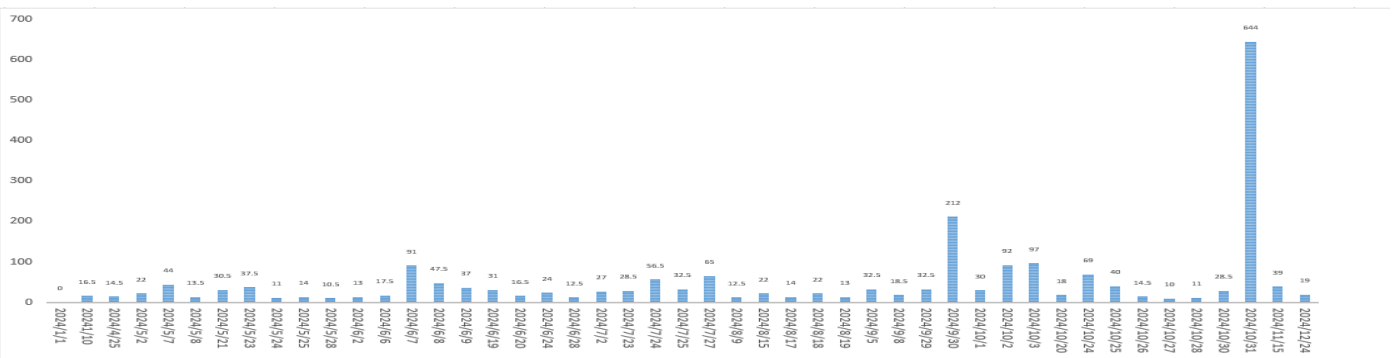


Fig11: Rainfall Statistics Table from January to December2024 Unit: day/mm

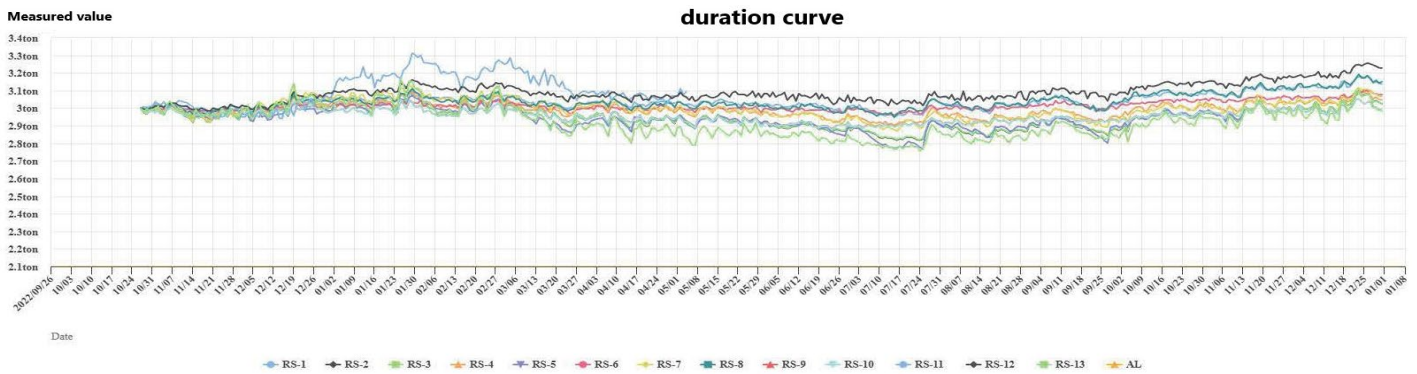


Fig 12: Strain Gauge Automated Monitoring of Prestress Variation Curve from October 31, 2022, to December 31, 2023.

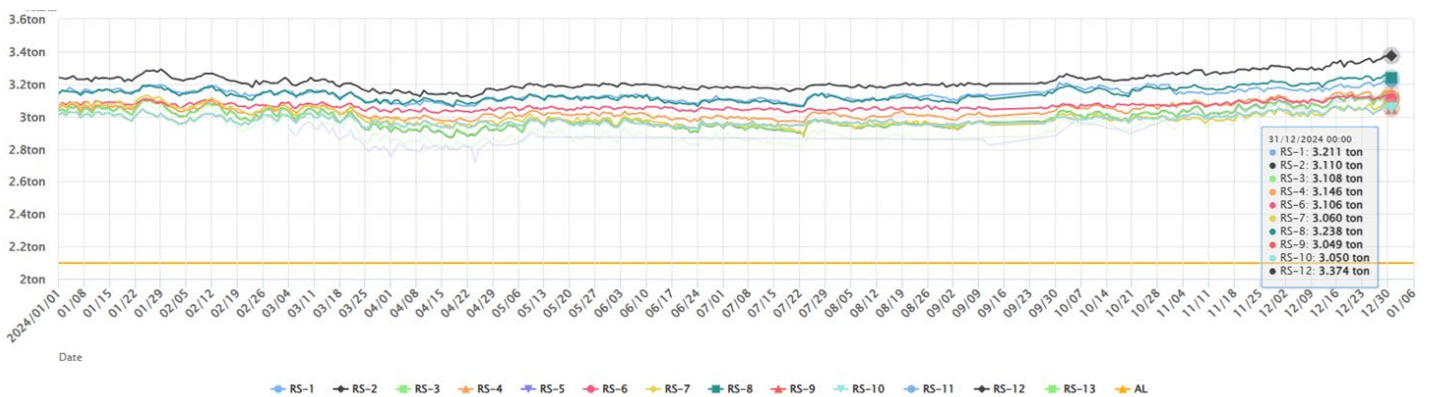


Fig13: Strain Gauge Automated Monitoring of Prestress Variation Curve from January to December 31, 2024

Item	Earthquake time	Longitude	Latitude	Scale	Depth
1	2022/12/8 00:54	121.601	23.7967	5.6	29.7
2	2022/12/15 12:03	121.845	23.7787	6.5	16.3
3	2023/2/8 18:49	121.549	23.4445	5.6	36.7
4	2023/6/11 20:25	122.492	24.2147	5.5	46.8
5	2023/8/13 09:43	121.473	20.5523	6	84
6	2023/9/5 17:30	120.385	23.5255	5.5	9.9
7	2023/9/12 19:03	121.08	19.2995	6.8	59.9
8	2023/9/18 21:21	125.583	25.9862	6.8	251.8
9	2023/10/11 18:36	121.244	23.2737	5.8	14.5
10	2023/10/24 07:05	122.624	24.0012	6.2	31.5
11	2023/11/1 00:54	121.57	23.458	5.5	39.1
12	2024/2/20 22:57	123.254	23.7213	5.7	58.9
13	2024/4/3 07:58	121.584	23.8607	7.2	22.5
14	2024/4/3 08:00	121.585	23.8075	5.7	30.7
15	2024/4/3 08:11	121.651	24.13	6.5	13.4
16	2024/4/3 08:35	121.706	24.2005	5.7	7.2
17	2024/4/3 08:46	121.7	24.1853	5.6	6.1
18	2024/4/3 08:50	121.572	23.8293	5.5	20.5
19	2024/4/3 09:39	121.773	23.8047	5.6	20.4
20	2024/4/3 10:14	121.976	24.1468	6.2	26.9
21	2024/4/21 10:40	121.675	23.4888	5.6	30
22	2024/4/22 17:08	121.546	23.7588	5.5	10
23	2024/4/22 18:50	121.514	23.7518	5.7	10
24	2024/4/22 22:11	121.52	23.7703	5.9	8.6
25	2024/4/23 02:26	121.663	23.7242	6	10
26	2024/4/23 02:32	121.543	23.8525	6.3	5.5
27	2024/4/23 04:49	121.579	23.723	5.9	10
28	2024/4/23 05:04	121.512	23.707	5.5	8
29	2024/4/23 05:19	121.541	23.783	5.7	10
30	2024/4/23 05:31	121.555	23.8525	5.7	8.1
31	2024/4/23 08:04	121.572	23.8352	6.1	11.7
32	2024/4/25 02:11	122.338	23.9128	5.6	18.5
33	2024/4/25 02:12	122.362	24.0335	5.5	24.1
34	2024/4/27 02:21	121.684	24.1902	6.1	24.9
35	2024/4/27 02:49	121.689	24.254	5.8	18.9
36	2024/5/6 17:45	121.562	23.7658	6	27.7
37	2024/5/6 17:52	121.541	23.7533	5.9	24.8
38	2024/5/10 15:45	121.834	24.2315	6	7.7
39	2024/6/1 01:10	121.533	24.0605	5.5	18.1
40	2024/6/23 22:27	121.619	23.8317	5.5	23.8
41	2024/6/29 14:39	122.423	25.3385	5.6	250.4
42	2024/7/27 19:21	121.162	21.826	5.6	49.5
43	2024/8/15 17:06	121.871	24.4027	5.8	12
44	2024/8/16 07:35	121.705	23.7828	6.3	19.4
45	2024/9/2 16:26	121.668	23.9287	5.5	23.9

3.3 Prestress Variations

Prestress values remained within safe limits (<30% loss) shown as table 4, confirming the system's effectiveness. shown as (Fig 11 、 And Fig12)

Table 4 Reference management values for this study

Pre-force rock bolt pre-force management value ^①	Pre-force loss management value ^②	Attention value ^③	Alert Value ^④	Action Value ^⑤
	2.1T ^②	Design tensile force=4.5T ^②	1.1 times the design tensile force=4.95T ^②	1.2 times the design tensile force =5.4T ^②

3.4 Rainfall Impact Analysis:

Heavy rainfall may lead to soil infiltration. Increasing the risk of soil erosion. The application of prestressed rock bolts can enhance slope stability. Prevent soil erosion . And integrate with a remote monitoring system. To provide timely disaster information. It can assist management units in determining slope safety. Heavy rainfall brings intense precipitation, increasing the moisture content of the slope. Potentially leading to an increase in pore water pressure. The prestressed rock bolt system can be designed with good drainage capacity. To reduce the accumulation of water .In addition to the above methods, we can also use the safety factor of (limit design) in the design stage:

$$F_s = \frac{\sum(c \cdot L + (W \cos \alpha - uL) \tan \phi)}{\sum W \sin \alpha} \dots\dots\dots(5)$$

Fs: Safety factor

c: Soil cohesion (kPa)

L: Sliding arc length (m)

W: Soil bar weight (kN/m)

α: Sliding arc angle.

u: Pore water pressure (kPa)

φ Friction angle of soil.

Refer to: Duncan & Wright (2005) 《Soil Strength and Slope Stability》

3.5 Seismic Impact Analysis:

The dynamic load caused by an earthquake can exert instantaneous pressure on the slope. The design of prestressed rock bolts should consider dynamic response. To enhance its seismic resistance. Additionally, Earthquakes may cause soil liquefaction or landslides. The stability design of prestressed rock bolts and the connection system can effectively withstand this risk.

3.6 Under the premise of no adverse effects.

Conduct thorough geological surveys and risk assessments. Ensure that the impacts of heavy rainfall and earthquakes are considered in the design and construction. Adopt appropriate materials and design methods. , This can ensure the effectiveness of the prestressed rock bolts and connection system under extreme weather and seismic conditions. [13,14]

3.7 Comparative Advantages Construction Efficiency: 20-30% reduction in time compared to traditional methods.

Table 3 Material comparison

^{①②}	Traditional method ^④ Free grid frame + anchor bar ^⑤	New technology Pre-force bolt and connection system ^③
Cement-based materials ^②	31,500 ^②	1,008 ^②
Main reinforcement materials ^②	12373 ^②	5,235.7 ^②
Other steel materials ^②	0.0 ^②	10,065 ^②
total ^②	43,873 ^②	16,308.7 ^②

IV. Conclusion

The tensioned rock anchor system, integrated with real-time monitoring, offers a sustainable and cost-effective solution for slope stabilization. Its success in mitigating rainfall and earthquake-induced risks underscores its potential for widespread adoption. This study explores the application of prestressed rock bolts and connection systems in slope protection. (15,16) It also compares the system with traditional free-frame shotcrete methods. The research results indicate that. The pre-force bolt and connection system has significant advantages in terms of duration, constructability., environmental impact and durability. For example. The prestressed rock bolts and connection system can save 20-30% of the construction duration. The construction flexibility is high. , Additionally, carbon emissions are reduced by more than 70% compared to traditional methods. In addition. The system components are lightweight, which makes transportation and installation easier. , It is easy to transport and install. It can also be integrated with long-term prestressing automation monitoring. This effectively monitors and ensures the safety of the slope. However . This study's case analysis is limited to specific regions and slope types. , Its applicability needs further verification.

V. Recommendations

- (1).Optimization: Tailor anchor parameters (length, spacing, prestress) to specific slope conditions.
- (2). Long-Term Monitoring: Expand studies to assess durability under varying environmental stresses.
- (3).Material Research: Explore alternatives like fiberglass or composites for enhanced performance.
- (4).Ecological Integration: Combine with vegetation to improve slope aesthetics and stability .

VI. Suggestion

It is recommended that, under suitable geological conditions and engineering requirements, The application of prestressed rock

bolts and connection systems should be promoted in slope protection engineering, under suitable geological conditions and engineering requirements. Additionally, the system should be tailored to different slope types and geological conditions. Optimize the design parameters of the prestressed rock bolts and connection systems. For example, parameters such as the length, spacing, and prestressing force of the rock bolts. Strengthen long-term monitoring of the prestressed rock bolts and connection systems. To evaluate their long-term performance and stability. Enhance monitoring Conduct more in-depth research., Explore the applicability of prestressed rock bolts and connection systems under different geological conditions. As well as their combined application with other slope protection measures For example. The durability of different anchor materials can be studied, such as comparing the performance of steel, fiberglass, or composite materials under various environmental conditions .and how to combine the pre-force rock bolt and connection system with the planting project, To enhance the ecological benefits of the slope.

REFERENCES

- [1] Anderson, S.A., Sitar, N., 1995. Analysis of rainfall-induced debris flows. *J. Geotech. Eng.* 121 (7), 544–552.
- in. or [50-mm] Cube Specimens), 2016, ASTM International, West Conshohocken, PA.
- [2] Chae, B.G., Lee, J.H., Park, H.J., Choi, J., 2015. A method for predicting the factor of safety of an infinite slope based on the depth ratio of the wetting front induced by rainfall infiltration. *Nat. Hazards Earth Syst. Sci.* 15, 1835–1849.
- [3] Choi, S.W., Lee, J., Kim, J.M. and Park, H.S. (2013). “Design and application of a field sensing system for ground anchors in slopes.” *Sensors*, 13(3), 3739-3752. <https://doi.org/10.3390/s130303739>
- [4] Huei - Long Wu (1991) 。 Study on Enhancing Slope land Use Control and Preventing Its Illegal and Unsuitable Development 。 *Journal of Chinese Soil and Water Conservation*, 22(1) , 85-94.
- [5] Hsien-Ter Chou (2003) 。 Threshold Conditions of Rainfall-induced Shallow Landslides with Cracks. *ournal of Chinese Soil and Water Conservation*, 34(4) , 347-352.
- [6] Giorgetti, A., Lucchi, M., Tavelli, E., Barla, M., G., Giovanni, C., Nicola, C.M., and Dardari, D. (2016). “A robust wireless sensor network for landslide risk analysis: System design, deployment, and field testing.” *IEEE Sensors Journal*, 16(16), 6374-6386. <https://doi.org/10.1109/JSEN.2016.2579263>
- [7] Intrieri, E., Gigli, G., Mugnai, F., Fanti, R., and Casagli, N. (2012). “Design and implementation of a landslide early warning system.” *Engineering Geology*, 147-148, 124-136. <https://doi.org/10.1016/j.enggeo.2012.07.017>
- [8] Jing Jing , Jingming Hou , Wen Sun, Guangzhao Chen, Yue Ma, Guo qiang Ji, Study on Influencing Factors of Unsaturated Loess Slope Stability under Dry-Wet Cycle Conditions. *Journal of Hydrology*, Volume 612, Part B, 2022, 128187, ISSN 0022-1694,
- [9] Koizumi, K., Hirata, K., Oda, K., Fujita, Y., Kamide, S., and Watanabe, T. (2012). “Slope disaster detection system using sensor networks and its field experiment evaluations.” *SICE Journal of Control Measurement and System Integration*, 5(1), 41-47. <https://doi.org/10.9746/jcmsi.5.41>
- [10] Koizumi, K., Murakami, K., Oda, K., Kamide, S., Konishi, T., Takemoto, M., and Fujiwara, Y. (2013b). “Evaluation of a field monitoring result for maintenance of slope along an expressway due to heavy rainfall.” *Proceedings of 2013 Kansai GeoSymposium*, Osaka, 155-160.
- [11] Li Weiyuana , Guo Xiangb , Luo Yuec , Yunnan Provincial Transportation Planning and Design Institute 、 Southwest Nonferrous Kunming Survey and Design (2012) .Highway slope stability calculations. *Theoretical Research on Urban Construction (Electronic Edition)* , (in Chinese)
- [12] Maneesha, V.R., Sangeeth K., and P. Venkat Rangan (2009). “Real-time wireless sensor network for landslide detection.” *Proceedings of the Third International Conference on Sensor Technologies and Applications*, Athens, 405-409. <https://doi.org/10.1109/SENSORCOMM.2009.67>
- [13] Smarsly, K., Georgieva, K., König, M., and Law, K.H. (2012). “Monitoring of slope movements coupling autonomous wireless sensor networks and web services.” *Proceedings of The First International Conference on Performance-Based Life-Cycle Structural Engineering*, Hong Kong. Smarsly, K., Georgieva, K., and König, M.. (2014). “An internetenabled wireless multi-sensor system for continuous monitoring of landslide processes.” *IACSIT International Journal of Engineering and Technology*, 6(6), 520-529. <https://doi.org/10.7763/IJET.2014.V6.752>
- [14] Subgrade slope stability analysis. *Heilongjiang Science and Technology Information*, (2008 36), 358-358。 36361 (in Chinese)
- [15] Takemoto, M., Koizumi, K., Fujiwara, Y., Morishita, H., and Oda, K. (2016). “Improvement of a slope disaster warning system for practical use.” *Japanese Geotechnical Society Special Publication*, 2(3), 196-200. <https://doi.org/10.3208/jgssp.VPS-05>
- [16] Zhao Chunqia, Wang Fengb, 304 Brigade of Hunan Nuclear Industry Geology Bureau, Changsha, Hunan 410000, Guangzhou Highway Survey and Design Co., Ltd., Guangzhou, Guangdong, 510080 (2008) 。